Draft version September 28, 2011
Preprint typeset using LaTeX style emulateapj v. 11/10/09

THE SPIN-DOWN OF SWIFT J1822.3−1606: A NEW GALACTIC MAGNETAR

M. A. Livingstone[1], P. Scholz, V. M. Kaspi, C.-Y. Ng
Department of Physics, Rutherford Physics Building, McGill University, 3600 University Street, Montreal, Quebec, H3A 2T8, Canada

and

Fotis P. Gavriil
NASA Goddard Space Flight Center, Astrophysics Science Division, Code 662, Greenbelt, MD 20771, USA and
Center for Research and Exploration in Space Science and Technology, University of Maryland Baltimore County, 1000 Hilltop Circle, Baltimore, MD 21250, USA

Draft version September 28, 2011

ABSTRACT

On 2011 July 14, a new magnetar candidate, Swift J1822.3−1606, was identified via a rate trigger on the *Swift*/Burst Alert Telescope. Here we present an initial analysis of the X-ray properties of the source, using data from the *Rossi X-ray Timing Explorer*, *Swift*, and the *Chandra X-ray Observatory*, spanning 2011 July 16 – September 22. We measure a precise spin period of $P = 8.43771963(5)$ s and a spin-down rate of $\dot{P} = 2.97(28) \times 10^{-13}$, at MJD 55761.0, corresponding to an inferred surface dipole magnetic field strength of $B = 5.1 \times 10^{13}$ G, the second lowest thus far measured for a magnetar, though similar to 1E 2259+586 as well as to several high-magnetic field radio pulsars. We show that the pulsed X-ray flux decay in the 2 – 10 keV band is best fit by an exponential with a time constant of 16.4±0.3 days. After increasing from ∼35% during the first week after the onset of the outburst, the pulsed fraction in the 2 – 10 keV band remained constant at ∼45%. We argue that these properties confirm this source to be a new member of the class of objects known as magnetars.

Subject headings: stars: magnetars — pulsars: individual (Swift J1822.3-1606) — stars: neutron — X-rays: bursts — X-rays: general

1. INTRODUCTION

On 2011 July 14, the *Swift*/Burst Alert Telescope (BAT) triggered on several bursts of hard X-ray emission from the direction of a previously unknown source, subsequently named Swift J1822.3−1606 (Cummings et al. 2011). The spin period of the new source was soon identified to be $P = 8.4377$ s (Göğüş et al. 2011) and observations with *Swift* X-ray Telescope (XRT) were used to further localize the position of the source (Pagani et al. 2011).

The simplest interpretation of these initial observations is that Swift J1822.3−1606 is a magnetar. However, because of suggested similarities between Swift J1822.3−1606 and the unusual Be X-ray binary J1626−5156, namely, a similar pulsed fraction and IR counterpart, it was suggested that perhaps Swift J1822.3−1606 is also a Be X-ray binary (Göğüş et al. 2011; Bandyopadhyay et al. 2011). This hypothesis was challenged by Halpern (2011), who, due to the lack of an optical counterpart (de Ugarte Postigo & Munoz-Darias 2011), argued that the properties of Swift J1822.3−1606 are in line with those of other magnetars, in particular, the transient magnetar XTE J1810−197. Here we report on timing and flux properties of Swift J1822.3−1606 that rule out a Be binary, and instead agree strongly with the magnetar identification.

Magnetars are neutron stars powered by the decay of extreme magnetic fields (Thompson & Duncan 1995; Thompson & Duncan 1996; Thompson et al. 2002). Soft Gamma-ray Repeaters (SGRs) and Anomalous X-ray Pulsars (AXPs) are thought to be observational manifestations of magnetars, and we refer to them as such here. Magnetars exhibit X-ray bursts, spin periods (P) in the relatively narrow range[2] of 2 – 12 s, and are observed to spin down with time. As inferred from P and spin-down rate $\dot{P}$ via the conventional vacuum dipole braking model that implies dipolar magnetic field strength $B = 3.2 \times 10^{19}(P\dot{P})^{1/2}$ G, their inferred dipole magnetic fields tend to be significantly larger than for classical pulsars, typically $B > 10^{14}$ G. Magnetars are also observed to display variability in nearly all of their observed properties: flux and pulsed flux variations, spectral variations, pulse profile variability, timing noise and glitches (e.g., see Mereghetti 2008; Rea & Esposito 2011, for reviews).

The true underlying distribution of magnetic field strengths of magnetars is an open question. The recent discovery of a magnetar with a very low inferred magnetic field of $B < 7.5 \times 10^{12}$ G (SGR 0418+5729; Rea et al. 2010), has raised the question of how low the dipolar field can be for magnetar-like activity to be observed. Moreover, the discovery of a magnetar-like outburst from the high-B rotation-powered pulsar (RPP) J1846−0258 (Gavriil et al. 2008; Kumar & Safi-Harb 2008) highlights the question of whether rotation-powered pulsars and magnetars represent distinct classes of object, or if magnetars represent the high-B tail of a single population.

In this Letter, we present analyses of *Rossi X-ray Timing Explorer* (*RXTE*), *Swift*, and *Chandra X-ray Observatory* (*CXO*) data. We perform a phase-coherent

[1] maggie@physics.mcgill.ca

[2] See the Magnetar Catalog: http://www.physics.mcgill.ca/∼pulsar/magnetar/main.html

timing analysis and show that the spin evolution is consistent with a constant spin-down rate. We present an analysis of the decay of the source's pulsed intensity after the outburst, and show that the pulsed fraction is steady after increasing during the first week after the outburst. We argue that these properties confirm that Swift J1822.3−1606 is a new Galactic magnetar.

2. OBSERVATIONS

2.1. *Swift Observations*

On 2011 July 14 at 12:47:47 UT the *Swift*/BAT triggered on a rate increase from the previously unknown source, Swift J1822.3−1606 (Cummings et al. 2011). The XRT began observing Swift J1822.3−1606 on 2011 July 15 at 17:43:20 UT. A total of 24 observations were taken with the XRT (target IDs 32033 and 32051). The observations span 67 days: 2011 July 15 – September 20 (MJD 55758 – 55824), for a total exposure time of 46 ks.

Cleaned *Swift* data in both windowed-timing (WT) mode with 1.8-ms time resolution and photon-counting (PC) mode with 2.5-s time resolution were downloaded from the *Swift* quick-look data archive[3]. For the lone PC mode observation, an annular source region with an outer radius of 20 pixels and an inner radius of 5 pixels was extracted. The inner radius was excluded because of pile-up. For the WT mode observations, a 16 pixel strip centered on the source was used. Events in the 2 – 10 keV energy range were then extracted from the reduced WT mode data for the timing analysis. The PC mode data have insufficient time resolution to be useful for timing.

2.2. *RXTE Observations*

Swift J1822.3−1606 data were obtained with the Proportional Counter Array (PCA; Jahoda et al. 2006) on board *RXTE*. The PCA consists of five xenon/methane proportional counter units (PCUs) sensitive to 2 – 60 keV photons, with an effective area of $\sim 6500\,\mathrm{cm}^2$ and a $\sim 1^\circ$ FWHM field of view. We downloaded 23 public *RXTE* observations of Swift J1822.3−1606 from the HEASARC archive[4] (observing program P96048). Data were collected in `GoodXenon` mode, which records the arrival time (1-μs resolution) and energy (256-channel resolution) of each event. The observations span 62 days: 2011 July 16 – September 16 (MJD 55758 – 55820), for a total exposure time of 119 ks.

For our timing analysis, we extracted 2 – 10 keV photons (because this produced high significance pulse profiles for individuals observations) from the top xenon layer of each PCU to reduce contamination from the particle background. Data from individual PCUs were then merged. When more than one observation occurred in a 24-hr period, we combined the data to produce better profiles.

2.3. *Chandra Observations*

CXO ACIS-S observations were made on 2011 July 27 (MJD 55769.2, ObsID 12612), August 4 (MJD 55777.1, ObsID 12613), and September 18 (MJD 55822.7, ObsID 12614) with net exposures of 15.0 ks, 13.7 ks, and 10.0 ks, respectively. All three observations were obtained in continuous clocking mode, with 2.85-ms time resolution. We carried out the data reduction using CIAO 4.3 with CALDB 4.4.3[5]. We reprocessed the data to retain events on the chip node boundary, then extracted the source counts from a 6″-width aperture and the 0.5–8 keV energy range for our timing analysis, and 2–8 keV for the pulsed fraction analysis.

3. ANALYSIS & RESULTS

3.1. *Phase-coherent Timing Analysis*

Our timing analysis of Swift J1822.3−1606 follows the common phase-coherent approach, in which we account for each rotation of the pulsar (see, for example Manchester & Taylor 1977) and utilized a combination of timing data from *RXTE*, *Swift*, and *Chandra*. For data from each telescope, events were reduced to barycentric dynamical time (TDB) at the solar system barycenter using the XRT position of RA=$18^\mathrm{h}\ 22^\mathrm{m}\ 18^\mathrm{s}$, Dec=$-16^\circ\,04'\,26.8''$ (J2000; Pagani et al. 2011) and the JPL DE200 solar system ephemeris. Events were then binned into time series with 31.25-ms time resolution.

Each *RXTE* (2 – 10 keV), *Swift* (2 – 10 keV), and *CXO* (0.5 – 8 keV) time series was folded with 64 phase bins using a frequency determined from a periodogram analysis. After finding an initial phase-coherent timing solution, we used this ephemeris to re-fold all the profiles to produce higher quality pulse Times Of Arrival (TOAs). For *RXTE* data, we found that using 128 phase bins created good pulse profiles with optimal TOA uncertainties. For *Swift* and *CXO* data, 64-bin profiles resulted in higher significance pulse profiles and good TOA uncertainties. 128- and 64-bin template profiles were created by aligning and summing all *RXTE* profiles.

To account for the different energy ranges and telescope responses between *RXTE*, *Swift*, and *CXO*, which result in small but significant differences in the profiles, we fit for a constant phase offset between TOAs obtained from different telescopes. We used a subset of the available data to fit for the phase offsets (MJD 55758 – 55781), which were then held fixed for the remainder of the timing analysis.

We searched for time variability in the pulse profile and found that individual profiles are consistent with the template in each case except for the first observation after the outburst (96048-02-01-00). In this case, the variation is subtle, at the ∼0.015 phase level. We accounted for this by multiplying the corresponding TOA uncertainty by three.

For each profile, we implemented a Fourier domain filter by using six harmonics in the cross-correlation procedure with the appropriate 64- or 128-bin template. Cross-correlation produces a TOA for each observation with a typical uncertainty of ∼27 ms (0.32% of P) for *RXTE* TOAs, ∼59 ms (0.70% of P) for *Swift* TOAs, and ∼23 ms (0.27% of P) for *CXO* TOAs. TOAs were fitted with the software package `TEMPO`[6]; parameters from this fit are given in Table 1.

The top panel of Figure 1 shows timing residuals with only spin-frequency (ν) fitted, while the bottom panel shows residuals with the frequency derivative ($\dot{\nu}$) also

[3] http://swift.gsfc.nasa.gov/cgi-bin/sdc/ql
[4] http://heasarc.gsfc.nasa.gov/docs/archive.html
[5] http://cxc.harvard.edu/ciao4.3
[6] http://www.atnf.csiro.au/people/pulsar/tempo/

fitted. Fitting $\dot{\nu}$ improves the RMS residuals by a factor of 1.8 and improves the ${\chi^2}_\nu/\nu$ from 3.66/44 to 1.14/43. Resulting phase residuals show minimal evidence for an unmodelled trend and fitting further parameters does not significantly improve the fit. The fitted values of ν and $\dot{\nu}$ imply a surface dipolar magnetic field of $B = 5.1{\times}10^{13}$ G.

3.2. *Pulsed Count-rate Evolution*

To measure the source intensity and decay after the outburst, we first checked for the presence of dust scattering rings, such as those observed around 1E 1547−5408 (Tiengo et al. 2010), because these will bias the inferred source count rate. We checked for deviations from the point-spread functions (PSFs) in the first *Swift* PC mode and *CXO* observations following the outburst. The radial profiles were well fit by the model PSFs, hence we found no evidence for dust scattering rings.

To measure the pulsed count rate for each *Swift* and *CXO* observation, the barycentered time series were folded with the ephemeris (see Table 1 and Section 3.1), with 16 phase bins. The pulsed count rate for each folded profile in the 2 – 10 keV energy range was then determined using a root-mean-squared (RMS) method. We calculate the RMS pulsed count rate using Fourier components as described in Dib et al. (2008), using 5 Fourier harmonics of the pulse profile. The pulsed fraction was then determined by dividing the pulsed count rate by the total source count rate.

To measure the pulsed count rate for *RXTE* data, we created phase-resolved spectra with 16 bins using the software program `fasebin`[7] to fold barycentered photons with the ephemeris (Table 1). We selected photons in the 2 – 10 keV energy range and from the top xenon detection layer. To minimize instrumental effects, we included only data from PCU2. PCU0 and PCU1 have lost propane layers, adversely affecting their particle background levels[8], and data available from PCU3 and PCU4 were minimal for this source. The RMS method with 5 harmonics was then used to measure the pulsed count rate. Because the PCA is not a focusing instrument the pulsed fraction could not be accurately determined from these data.

Figure 2 shows the evolution of the pulsed source intensity (top panel, as measured with *Swift* and *RXTE*), and the pulsed fraction (bottom panel, as measured with *Swift* and *CXO*). We present here the pulsed source intensity evolution only in terms of count rate, instead of fluxes. A detailed spectral analysis will follow in a subsequent paper. To describe this pulsed intensity decay quantitatively, we fit the pulsed count-rate evolution of Swift J1822.3−1606 in the 2 – 10 keV energy range with an exponential decay. Pulsed count rates from a given source for *RXTE* and *Swift* are different owing to instrumental effects (e.g. effective area), but should be offset only by a constant, and trends should be the same between instruments (as is observed here). Thus, *RXTE* PCA pulsed count rates were scaled to the *Swift* XRT pulsed count rates. The scaling factor was chosen to be that which minimized the residuals of the fit to the pulsed count rates. The exponential decay is described by $F(t) = F_p \exp^{-(t-t_0)/\tau} + F_q$ where F_p is the peak count rate, F_q is the count rate in quiescence, t_0 is the time of the BAT trigger in MJD and τ is the decay timescale in days. With a χ^2_ν of 2.69 for 41 degrees of freedom, the best-fit decay timescale is 16.4 ± 0.3 days. A power-law model was also fit to the decay, but it provided a much worse fit with a χ^2_ν of 79 for 41 degrees of freedom.

The bottom panel of Figure 2 shows the evolution of the 2 – 10 keV pulsed fraction of Swift J1822.3−1606 for *Swift* and *CXO* data. The pulsed fraction appears to have increased from ∼35% immediately after the outburst until about one week after the BAT trigger. It then remained constant at ∼45%.

4. DISCUSSION

The regular spin-down we report for Swift J1822.3−1606, together with a pulsed flux decay similar to that seen in other magnetar outbursts, demonstrates that this source indeed shares critical properties with other known magnetars; we hence classify it as such. The inferred surface dipole B for Swift J1822.3−1606 of 5.1×10^{13} G is smaller than those of all but one confirmed magnetar, SGR 0418+5729 (Rea et al. 2010), though it is very close to that of AXP 1E 2259+586 ($B = 5.9 \times 10^{13}$ G; Gavriil & Kaspi 2002). As for the latter, Swift J1822.3−1606's B is similar to that measured for several RPPs, including the lone identified magnetically active RPP, PSR J1846−0258 which has $B = 4.9 \times 10^{13}$ G (Gotthelf et al. 2000). Although enhanced spin-down could be present if the source suffered a large glitch at the outburst (e.g. Kaspi et al. 2003), the duration of our observations of Swift J1822.3−1606 (64 days) significantly exceeds the glitch recovery time scales measured in previous large magnetar glitches, so any contamination is likely to be small.

Interestingly, the most recently discovered magnetars (including SGR 0418+5729 and Swift J1822.3−1606, but also SGRs 0501+4516, 1833−0832 and Swift J1834.9−0846; Göğüş et al. 2010a,b; Rea et al. 2010, Kuiper & Hermsen 2011) all have $B \lesssim 1 \times 10^{14}$ G, effectively lowering the 'average' inferred B-field for magnetars. This raises the question of what is the true distribution of magnetar field strengths. In Figure 3, we plot the distributions of the periods and inferred surface dipolar magnetic fields of all confirmed magnetars, as well as of all known $B > 10^{12}$ G radio pulsars.

The P distribution of magnetars remains narrow, spanning less than an order of magnitude, in great contrast to those of radio pulsars. We note that the period distribution for magnetars is statistically consistent with being flat; a fit to the histogram mean yields a ${\chi^2}_\nu$ of 0.63. This is somewhat surprising and needs to be addressed in any future population studies. The B distribution for observed magnetars, by contrast, appears more peaked, even with the relatively low B we have measured for Swift J1822.3−1606, albeit with the possible low tail represented by SGR 0418+5729. If the magnetars represent the high-B tail of the B distribution of all non-recycled neutron stars, then their peaked B distribution may indicate that burst rates of these sources fall rapidly with decreasing B, since the primary mechanism for their discovery is through their bursting behavior, particularly with the *Swift* BAT and *Fermi* GBM. This would be broadly consistent with the theoretical findings of Perna & Pons

[7] http://heasarc.nasa.gov/docs/xte/recipes/fasebin.html
[8] http://heasarc.gsfc.nasa.gov/docs/xte/pca_history.html

(2011), who calculate expected burst rates in neutron stars and show that all neutron stars can show magnetar-like bursts, though the burst rate drops with decreasing B and increasing age. That the distribution of radio pulsars plummets rapidly above $B \sim 10^{13}$ G could genuinely be due to fall-off in the intrinsic distribution, or to smaller radio beams for these preferentially longer-period pulsars, but may also indicate that radio emission is harder to produce at higher B (e.g. Baring & Harding 2001). Although radio emission has been observed for three magnetars (Camilo et al. 2006, 2007; Levin et al. 2010), their radio spectra and radiative stabilities are vastly different than for conventional radio pulsars, suggesting a distinct emission mechanism. Hence, if indeed we can 'unify' radio pulsars and magnetars as described above, we expect the lowest B magnetars to be the likeliest to produce observable traditional radio-pulsar-like radio emission, and the highest B RPPs to be the likeliest to show magnetar-like X-ray outbursts. The latter is consistent with the behavior of PSR J1846−0258 (Gavriil et al. 2008), while as yet, there is no evidence to support the former prediction. Such a unification would also suggest that there exists a large population of as yet undetected $B \sim 10^{13}$ G neutron stars that could be one day detected via their occasional magnetar-like bursts.

The characteristic age ($\tau_c = P/2\dot{P}$) for Swift J1822.3−1606 is 450 kyr, comparable to that of AXP 1E 2259+586 but much larger than for all other magnetars, except for SGR 0418+5729 (>24 Myr). 1E 2259+586 is firmly associated with the supernova remnant CTB 109 which is thought to have an age of ∼9 kyr (Sasaki et al. 2004), much smaller than the AXP's characteristic age of 250 kyr. This demonstrates that τ_c for magnetars can be unreliable true age indicators, which perhaps can be ascribed to epochs of greater spin-down torque early in the star's history, when the dipolar field was larger. Indeed this hypothesis can also explain the large τ_c of SGR 0418+5729, although the latter's greater distance from the Galactic Plane suggests it may indeed be the oldest known magnetar (but see Alpar et al. 2011, for an alternative discussion). Turolla et al. (2011) suggest that the observed properties of SGR 0418+5729 are consistent with it being an aged magnetar in which the external B has decayed significantly. Further evidence for SGR 0418+5729 being older than other magnetars includes lower energy bursts and a very low quiescent luminosity. Whether Swift J1822.3−1606 more closely resembles SGR 0418+5729 or 1E 2259+586 remains to be seen. The measurement of its flux in quiescence and the discovery of an associated supernova remnant would help resolve this issue.

The post-outburst pulsed count rate evolution of Swift J1822.3−1606 is best characterized by an exponential decay with timescale of 16.4±0.3 days. This is similar to what has been observed after several other magnetar outbursts (e.g. Rea et al. 2009; Gotthelf & Halpern 2005; Gavriil et al. 2008), though power-law decays are also common (e.g. Woods et al. 2001; Kouveliotou et al. 2003). Lyubarsky et al. (2002) predicted power-law decays in magnetar outbursts assuming crustal cooling following an impulsive heat injection. Beloborodov & Thompson (2007), by contrast, considered magnetar outbursts as a result of sudden twisting of magnetic field lines in the magnetosphere, with the relaxation a result of their untwisting. In this model, the relaxation is predicted to be approximately linear, a functional form observed in one outburst of 1E 1048.1−5937 (Dib et al. 2009). Beloborodov (2009) showed that other functional forms for the decay, including exponential, are possible, as the untwisting is predicted to be strongly non-uniform, being erased by a propagating 'front' whose speed depends on the initial twist configuration. The diversity in functional forms for the flux decays of magnetars hence favors the model put forth by Beloborodov (2009).

We thank the *Chandra* and *Swift* teams for their work in scheduling Target of Opportunity observations. This research made use of data obtained from the High Energy Astrophysics Science Archive Research Center Online Service, provided by NASA-GSFC. V.M.K. holds the Lorne Trottier Chair in Astrophysics and Cosmology and a Canada Research Chair in Observational Astrophysics. This work is supported by NSERC via a Discovery Grant, by FQRNT, by CIFAR, and a Killam Research Fellowship. CYN is a Tomlinson postdoctoral fellow and a CRAQ postdoctoral fellow.

REFERENCES

Alpar, M. A., Ertan, Ü., & Çalışkan, Ş. 2011, ApJ, 732, L4
Bandyopadhyay, R. M., Lucas, P. W., & Maccarone, T. 2011, The Astronomer's Telegram, 3502
Baring, M. G. & Harding, A. K. 2001, ApJ, 547, 929
Beloborodov, A. M. 2009, ApJ, 703, 1044
Beloborodov, A. M. & Thompson, C. 2007, ApJ, 657, 967
Camilo, F., Ransom, S., Halpern, J., Reynolds, J., Helfand, D., Zimmerman, N., & Sarkissian, J. 2006, Nature, 442, 892
Camilo, F., Ransom, S. M., Halpern, J. P., & Reynolds, J. 2007, ApJ, 666, L93
Cummings, J. R., Burrows, D., Campana, S., Kennea, J. A., A., K. H., , Palmer, D. M., T., S., & Zane, M. 2011, GRB Circular Network, 12159
de Ugarte Postigo, A. & Munoz-Darias, T. 2011, The Astronomer's Telegram, 3518, 1
Dib, R., Kaspi, V. M., & Gavriil, F. P. 2008, ApJ, 673, 1044
—. 2009, ApJ, 702, 614
Gavriil, F. P., Gonzalez, M. E., Gotthelf, E. V., Kaspi, V. M., Livingstone, M. A., & Woods, P. M. 2008, Science, 319, 1802
Gavriil, F. P. & Kaspi, V. M. 2002, ApJ, 567, 1067
Gotthelf, E. V. & Halpern, J. P. 2005, ApJ, 632, 1075
Gotthelf, E. V., Vasisht, G., Boylan-Kolchin, M., & Torii, K. 2000, ApJ, 542, L37
Göğüş, E., et al. 2010a, ApJ, 718, 331
Göğüş, E., Kouveliotou, C., & Strohmayer, T. 2011, The Astronomer's Telegram, 3491
Göğüş, E., Woods, P. M., Kouveliotou, C., Kaneko, Y., Gaensler, B. M., & Chatterjee, S. 2010b, ApJ, 722, 899
Halpern, J. 2011, GRB Coordinates Network, 12170, 1
Jahoda, K., Markwardt, C. B., Radeva, Y., Rots, A. H., Stark, M. J., Swank, J. H., Strohmayer, T. E., & Zhang, W. 2006, ApJS, 163, 401
Kaspi, V. M., Gavriil, F. P., Woods, P. M., Jensen, J. B., Roberts, M. S. E., & Chakrabarty, D. 2003, ApJ, 588, L93
Kouveliotou, C., Eichler, D., Woods, P. M., Lyubarsky, Y., Patel, S. K., Göğüş, E., van der Klis, M., Tennant, A., Wachter, S., & Hurley, K. 2003, ApJ, 596, L79
Kuiper, L. & Hermsen, W. 2011, The Astronomer's Telegram, 3577, 1
Kumar, H. S. & Safi-Harb, S. 2008, ApJL, 678, L43
Levin, L., et al. 2010, ApJ, 721, L33
Lyubarsky, Y., Eichler, D., & Thompson, C. 2002, ApJ, 580, L69

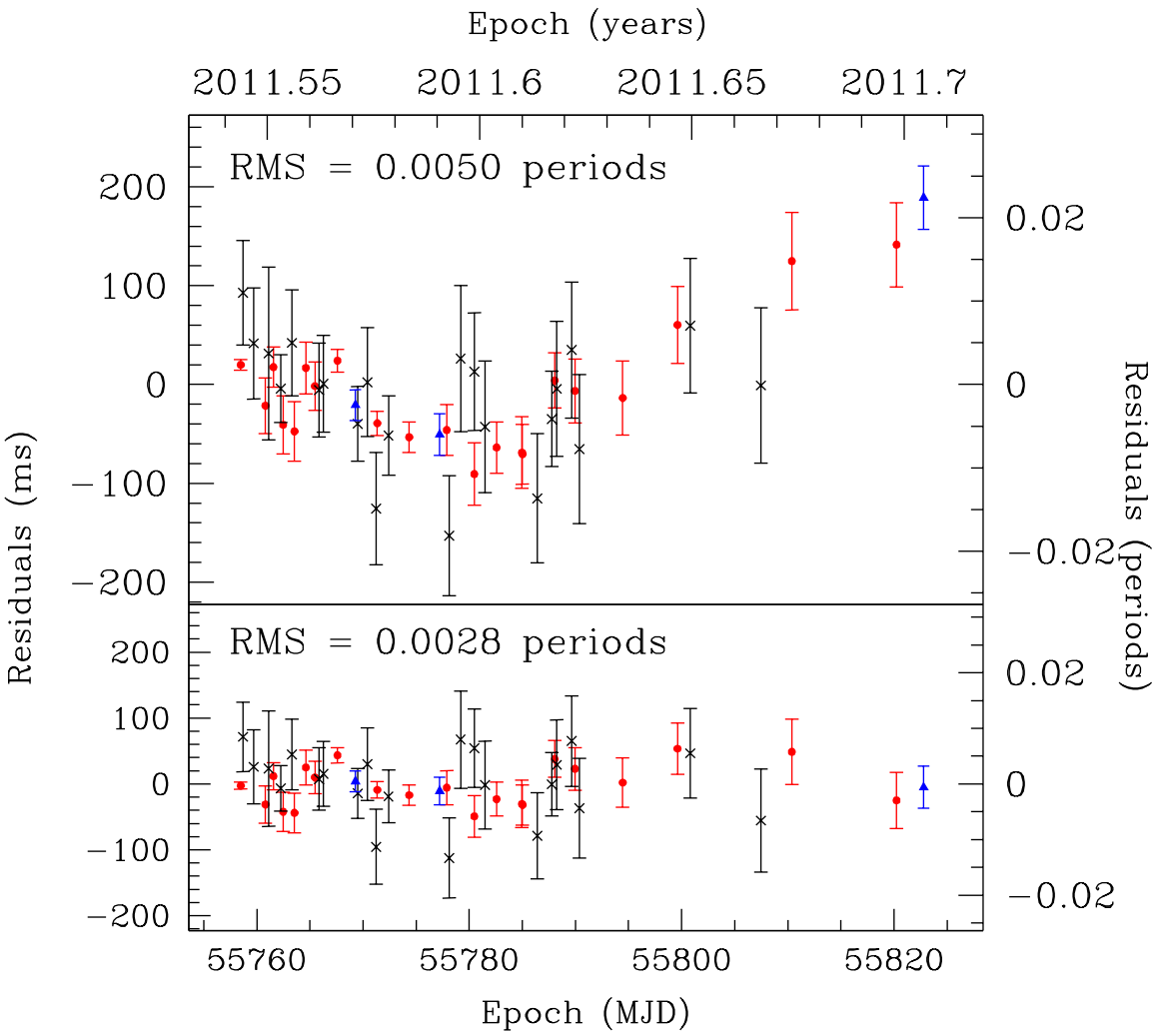

Figure 1. X-ray timing residuals for Swift J1822.3−1606 spanning 2011 July 16 – September 22. *RXTE* points are shown as filled red circles, *Swift* points are black crosses, and *CXO* points are blue triangles. The top panel shows residuals with only ν fitted, while the bottom panel shows timing residuals with $\dot{\nu}$ also fitted. Parameters from this fit are given in Table 1.

Manchester, R. N. & Taylor, J. H. 1977, Pulsars (San Francisco: Freeman)
Mereghetti, S. 2008, A&A Rev., 15, 225
Pagani, C., Beardmore, A. P., & Kennea, J. A. 2011, The Astronomer's Telegram, 3493
Perna, R. & Pons, J. A. 2011, ApJ, 727, L51
Rea, N. & Esposito, P. 2011, in High-Energy Emission from Pulsars and their Systems, ed. D. F. Torres & N. Rea, 247
Rea, N., et al. 2010, Science, 330, 944
Rea, N., et al. 2009, MNRAS, 396, 2419
Sasaki, M., Plucinsky, P. P., Gaetz, T. J., Smith, R. K., Edgar, R. J., & Slane, P. O. 2004, ApJ, 617, 322
Thompson, C. & Duncan, R. C. 1995, MNRAS, 275, 255
Thompson, C. & Duncan, R. C. 1996, ApJ, 473, 322
Thompson, C., Lyutikov, M., & Kulkarni, S. R. 2002, ApJ, 574, 332
Tiengo, A., et al. 2010, ApJ, 710, 227
Turolla, R., Zane, S., Pons, J. A., Esposito, P., & Rea, N. 2011, ApJ, in press. arXiv:1107.5488
Woods, P. M., Kouveliotou, C., Göğüş, E., Finger, M. H., Swank, J., Smith, D. A., Hurley, K., & Thompson, C. 2001, ApJ, 552, 748

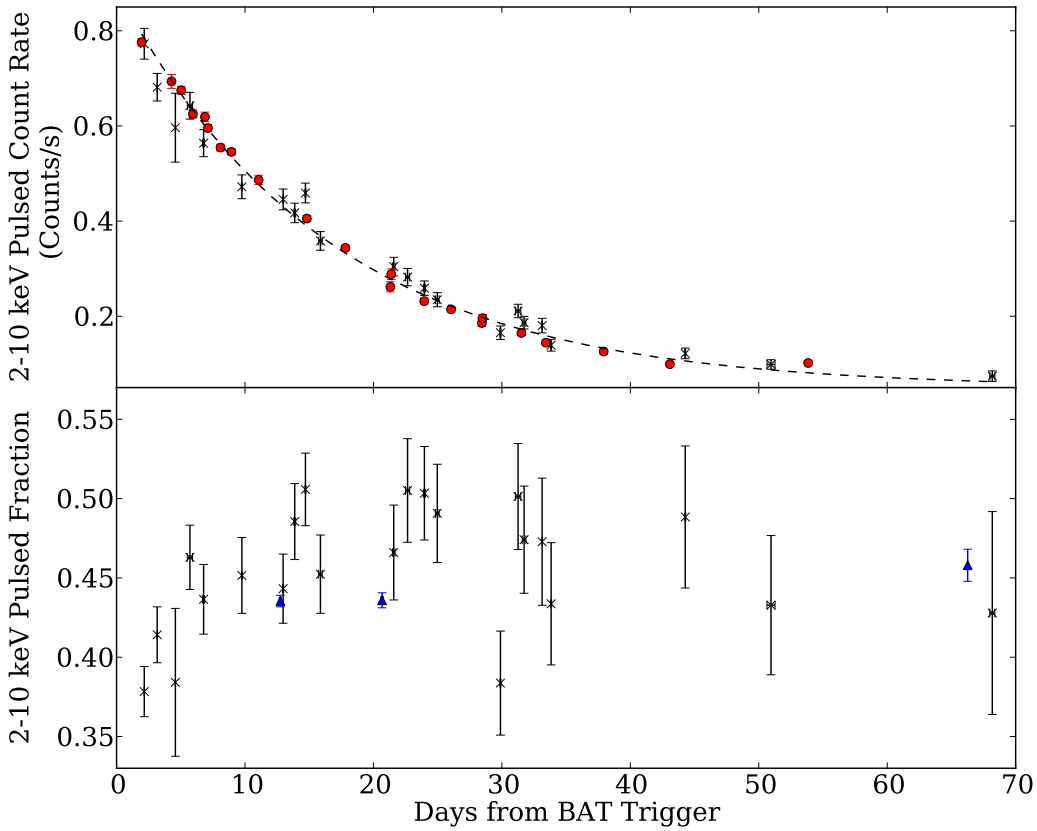

Figure 2. Top: Pulsed count rate evolution of Swift J1822.3−1606 in the 2 – 10 keV energy range following its outburst. *Swift* data are shown as black crosses, *RXTE* data are filled red circles. The dashed line indicates the best-fit exponential decay with $\tau = 16.4 \pm 0.3$ days. Bottom: Pulsed fraction measurements in the 2 – 10 keV with *Swift* data as black crosses and *CXO* data as blue triangles.

Table 1
Spin Parameters for Swift J1822.3−1606.

Parameter	Value
Dates (Modified Julian Day)	55758 – 55822
Epoch (Modified Julian Day)	55761.0
Number of TOAs - *RXTE*	21
Number of TOAs - *Swift*	22
Number of TOAs - *CXO*	3
ν (Hz)	0.1185154336(8)
$\dot{\nu}$ (Hz^2)	$-4.2(4) \times 10^{-15}$
RMS residuals (ms)	23.4
RMS residuals (periods)	0.0028
Derived Parameters	
P (s)	8.43771963(5)
$\dot{P}$	$2.97(28) \times 10^{-13}$
Surface Dipolar Magnetic Field, B (G)	$5.1(2) \times 10^{13}$
Spin-down Luminosity, $\dot{E}$ (erg s^{-1})	$2.0(2) \times 10^{31}$
Characteristic age, τ_c (kyr)	450(40)

Note. — Uncertainties are formal 1σ `TEMPO` errors.

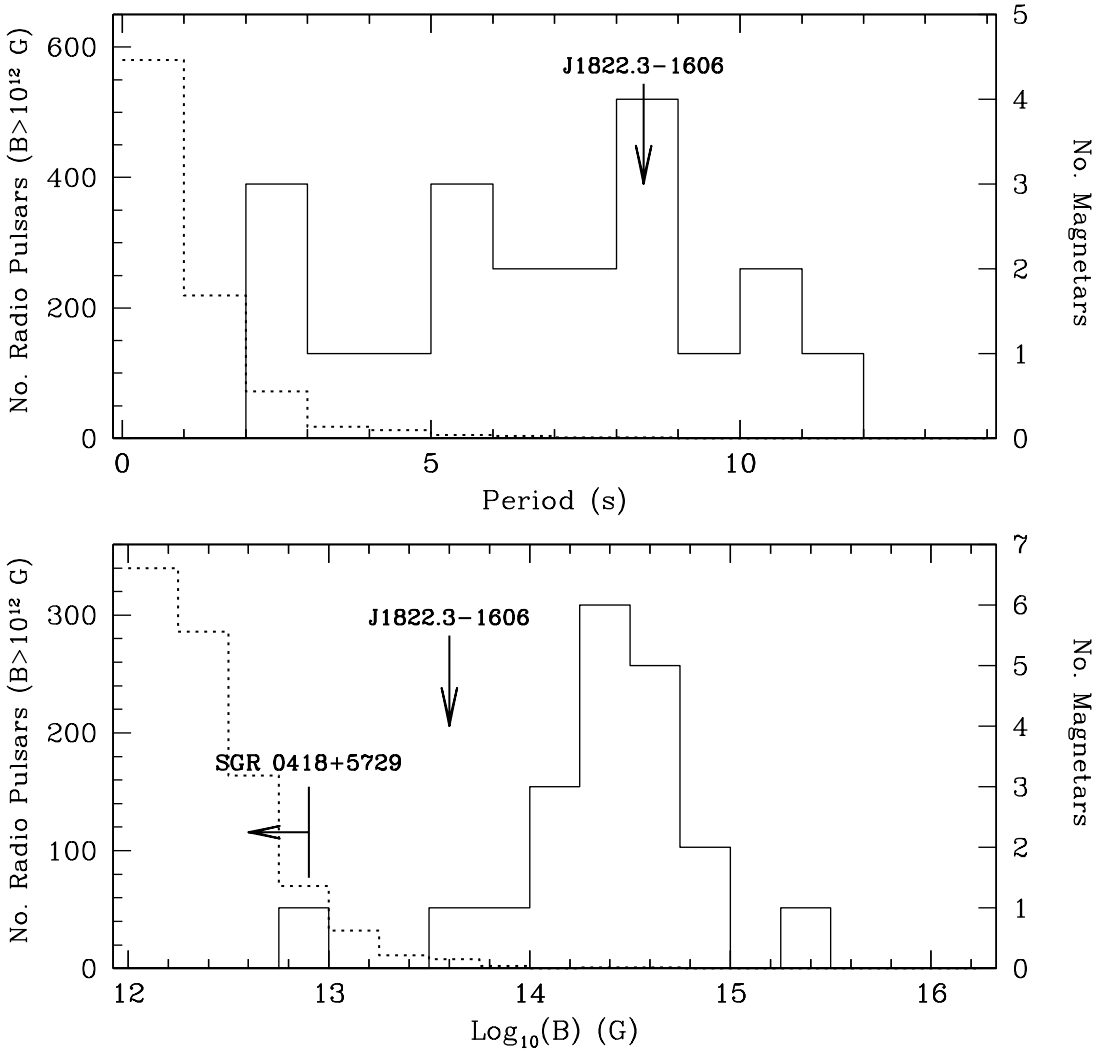

Figure 3. (Top) Histograms of the spin periods of observed magnetars (for which $\dot{P}$ has also been measured; see the online magnetar catalog, http://physics.mcgill.ca/∼magnetar/main.html; solid) and known radio pulsars having inferred $B > 10^{12}$ G (from the ATNF pulsar catalog at http://www.atnf.csiro.au/research/pulsar/psrcat/; dotted). Swift J1822.3−1606 is indicated. Note the different vertical axes for the radio pulsars (left) and magnetars (right). (Bottom) Histograms of the inferred B-field strength of the same magnetars (solid) and the same radio pulsars (dotted). Swift J1822.3−1606 is indicated, as is the upper limit for SGR 0418+5729 (Rea et al. 2010). Note again the different vertical axes.